

# $\alpha$ -attractor potentials in loop quantum cosmology

G. L. L. W. Levy<sup>1,\*</sup> and Rudnei O. Ramos<sup>2,†</sup>

<sup>1</sup>*Centro Brasileiro de Pesquisas Físicas – CBPF, Rio de Janeiro, RJ, Brasil,*

<sup>2</sup>*Departamento de Física Teórica, Universidade do Estado do Rio de Janeiro, 20550-013 Rio de Janeiro, RJ, Brazil*

We perform in this work an analysis of the background dynamics for  $\alpha$ -attractor models in the context of loop quantum cosmology. Particular attention is given to the determination of the duration of the inflationary phase that is preceded by the quantum bounce in these models. From an analysis of the general predictions for these models, it is shown that we can be able to put constraints in the parameter  $\alpha$  of the potentials and also on the quantum model itself, in special the Barbero-Immirzi parameter.

## I. INTRODUCTION

Building a theory of quantum gravity is still a challenge. Among the proposals, loop quantum gravity (LQG), which is a background independent and nonperturbative approach for quantizing general relativity (for reviews, see, e.g. Refs. [1–3]) has been widely investigated in the past 30 years or so. Meanwhile, the physical implications of LQG make use of its loop quantization techniques to cosmological models, namely loop quantum cosmology (LQC), which is the symmetry reduced version of LQG [2, 4–9]. In LQC, the quantum effects at the Planck scale are able to produce a bounce that results as a consequence of the repulsive quantum geometrical effects and, hence, effectively resolving the singularity issue of classical general relativity.

Making predictions concerning the inflationary phase that can be preceded by a quantum bounce has attracted quite some interest recently. Interestingly, it has been shown that in LQC that inflation can occur quite naturally and it is in general a strong attractor when a scalar field is the main ingredient of the energy density. This characteristics of LQC has been confirmed and studied in details in many recent works [10–15]. These works have shown that in LQC models with a kinetic energy dominated bounce lead to an almost inevitably inflationary phase following the bounce phase.

The discussion of the inflationary phase after the quantum bounce in LQC has been mostly studied following two lines of thoughts on how and when the initial conditions should be taken. One line of thought assumes that the initial conditions can be appropriately taken at the bounce [10–17]. Another school assumes that the appropriate moment to take the initial conditions would be deep inside the contracting phase before the bounce [18–22]. Both lines of thought lead to the conclusion that inflation is in general a strong attractor, however, in the latter case, when taking initial conditions deep in the contracting phase, it has been further demonstrated that not only inflation is highly probable, but that the duration of inflation itself can be predicted using simple analytical

methods as has been shown in Ref. [23]. Having a way of making predictions concerning the inflationary phase is quite important when comparing and contrasting different inflationary models with the observations.

In the present work, we make use of the method developed in Ref. [23] and apply it to the study of the dynamics for the  $\alpha$ -attractor type of potentials [24–26]. We focus in particular to the bouncing dynamics and the subsequent transition (pre-inflation phase) and inflationary phases following the quantum bounce in LQC. For different values of parameters in these potentials, we verify whether they can produce not only a sufficient number of  $e$ -folds such as to solve the usual big bang problems but also to be compatible with the observational predictions for these type of models, e.g. the tensor-to-scalar ratio and spectral tilt of the scalar perturbations. We note that the pre-inflationary dynamics in LQC for this class of potentials has also been studied previously in Refs. [15, 27] by adopting the school of thought of taking the initial conditions at the instant of the bounce, as proposed e.g. in Ref. [16]. In this approach, the authors of those references have then checked which initial conditions at the bounce would be able to lead to a sufficient duration of inflation in different  $\alpha$ -attractor models. Here, however, we follow the second line of thought, which argues that the appropriate instant for taking the initial conditions should be in the contracting phase and well before the bounce, as initially proposed in Ref. [18]. As already commented above, this has the additional advantage of making possible to make precise predictions for what should be the actual duration of inflation and avoids the arbitrariness of the former line of thought, of which initial condition should one actually take at the bounce instant.

The interest in considering the  $\alpha$ -attractor type of potentials is because they are a well-motivated class of inflationary potentials which are able to lead to universal predictions for large-scale observables that are largely independent of the details of the inflationary potential. Furthermore, they lead to predictions that lie close to the center of current observational bounds on the primordial power spectra [28, 29]. Let us recall that the Starobinsky potential [30], which is shown to fit quite well the current observations, is a particular case of an  $\alpha$ -attractor type of potential.

---

\* guslevy9@hotmail.com

† rudnei@uerj.br

We have organized this paper as follows. In Sec. II we briefly review the  $\alpha$ -attractor, in particular the T-, E-, and  $n = 2$  models which are considered in this work. In Sec. III we present the structure of LQC for developing the background dynamics and summarize the methods developed in Ref. [23], which are used in the present study. Our main results are presented in Sec. IV, where we study the background dynamics of the T-, E- and  $n = 2$  models, which includes the bouncing, pre-inflation and inflation phases and present the predictions that we obtain for these models. We also contrast our results with the previous ones obtained when considering initial conditions taken at the bounce instant. We use these results to constrain the  $\alpha$  parameter of the potentials and also the Barbero-Immirzi parameter when considering it as a free parameter in LQC. Finally, in Sec. V, we present our conclusions. Relevant technical details used in our analysis are also given in one appendix.

## II. THE $\alpha$ -ATTRACTOR POTENTIALS

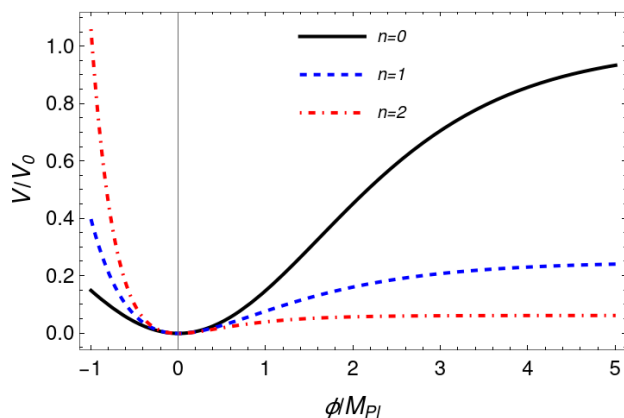


FIG. 1. The  $\alpha$ -attractor potential cases considered in this work. The parameter  $\alpha$  was set to the value  $\alpha = 1$ .

In this paper, we consider the following class of  $\alpha$ -attractor potentials given by [27, 31, 32]

$$V(\phi) = V_0 \frac{\left[ \tanh\left(\frac{\phi}{\sqrt{6\alpha} M_{\text{Pl}}}\right) \right]^2}{\left[ 1 + \tanh\left(\frac{\phi}{\sqrt{6\alpha} M_{\text{Pl}}}\right) \right]^{2n}}, \quad (2.1)$$

where  $M_{\text{Pl}} = m_{\text{Pl}}/\sqrt{8\pi}$  is the reduced Planck mass and  $m_{\text{Pl}} = 1.22 \times 10^{19}$  GeV is the Planck mass,  $\alpha$  is a dimensionless positive constant. The value of the power  $n$  parameterizes different classes of  $\alpha$ -attractor potentials. We will work with the cases where  $n = 0, 1, 2$ . For instance, for  $n = 0$ , in the literature, this potential is called the T-model [25, 33, 34]. The case with  $n = 1$  is known as the E-model and it is a generalization

of the Starobinsky model [30], which is obtained when  $\alpha = 1$ . In Eq. (2.1), the value of  $V_0$  is the normalization of the potential, which is fixed by the amplitude of the CMB scalar power spectrum for given values of  $n$  and  $\alpha$  (see the Appendix A for details). These type of potentials are well motivated for describing dark energy models to explain the late time cosmic acceleration [35] and they are also forms of potentials representing a limiting case of more general modified gravity theories, like the Starobinsky form. For large values of  $\alpha$  the models resemble monomial potentials [25] and if  $\phi \ll M_{\text{Pl}}$  the potentials approach a quadratic form, while for  $\phi \gg M_{\text{Pl}}$  they approach a constant (flatten) form. The three cases we will consider,  $n = 0, 1$  and  $2$  are shown in Fig. 1 for illustration.

These potentials also represent robust inflationary models when regarding their predictions. When compared with the observational constraints, like with the spectral tilt  $n_s$  and the tensor-to-scalar ratio  $r$ , they are able to fit well the data. For instance, when  $\alpha \ll 1$  and large number of  $e$ -folds of inflation they lead to [36] (see also Appendix A for details)

$$n_s \simeq 1 - \frac{2}{N_*}, \quad (2.2)$$

and

$$r \simeq \alpha \frac{12}{N_*^2}, \quad (2.3)$$

where  $N_*$  is the number of  $e$ -folds corresponding to the scales crossing the Hubble radius relevant to CMB, typically corresponding to  $N_* = 50 - 60$   $e$ -folds before the end of inflation, depending on the reheating history [37]. In the absence of running, the Planck data measure the spectral index to be [28]

$$n_s = 0.9649 \pm 0.0042, \quad (2.4)$$

while the recent data analysis of the BICEP, Keck Array combined with that from Planck data places the upper bound on the tensor-to-scalar ratio [38]

$$r < 0.036, \quad \text{at } 95\%CL. \quad (2.5)$$

In the Appendix A we show the behavior of both  $r$  and  $n_s$  for the three types of  $\alpha$ -attractors studied here and which are valid for any value of  $\alpha$ . It is found that the most constraining condition comes from the tensor-to-scalar ratio, giving the upper bounds on  $\alpha$ , obtained, e.g. at the lowest value of  $N_* = 50$ ,

$$\alpha \lesssim \begin{cases} 10, & \text{for } n = 0, \\ 17, & \text{for } n = 1, \\ 67, & \text{for } n = 2. \end{cases} \quad (2.6)$$

### III. BACKGROUND DYNAMICS IN LQC

In LQC, the Friedmann equation is modified by the quantum effects and given by [7, 16]

$$H^2 = \frac{8\pi}{3m_{\text{Pl}}^2} \rho \left(1 - \frac{\rho}{\rho_{\text{cr}}}\right), \quad (3.1)$$

where  $\rho$  is the total energy density and  $\rho_{\text{cr}}$  is the critical energy density at which the bounce happens. For  $\rho \ll \rho_{\text{cr}}$  we recover general relativity as expected. The critical energy density is given by

$$\rho_{\text{cr}} = \frac{\sqrt{3}m_{\text{Pl}}^4}{32\pi^2\gamma^3}, \quad (3.2)$$

and with  $\gamma$  being the Barbero-Immirzi parameter. It is common in the literature of LQC to assume the Barbero-Immirzi parameter as given by the value  $\gamma \simeq 0.2375$ , which is motivated by black hole entropy calculations [39]. However, many authors prefer to consider  $\gamma$  to be a free parameter in quantum gravity theories (see, e.g. Refs. [40–42]). In our analysis, to be performed in the next sections, we will consider both point of views. In particular, when taking  $\gamma$  as a free parameter, we will explore how the type of potentials we are considering in LQC can be made consistent with the observations. This will allow us to put an upper bound in  $\gamma$ .

In this present paper, we work with the dynamics of one scalar field  $\phi$ , the inflaton, with the potential as given by Eq. (2.1) in the three cases mentioned previously, the T-model ( $n = 0$ ) the E-model ( $n = 1$ ) and the case with  $n = 2$ . In the Lemaître-Friedmann-Robertson-Walker (LFRW) metric, the background evolution for the inflaton is given by

$$\ddot{\phi} + 3H\dot{\phi} + V_{,\phi} = 0, \quad (3.3)$$

where  $V_{,\phi} \equiv dV(\phi)/d\phi$  is the derivative of the inflaton's potential.

As stated in the introduction, we follow the background dynamics starting from the contracting phase, well before the bounce, where the initial conditions are set, and follow the dynamics of the inflaton through the bounce, along the postbounce expanding pre-inflationary phase, the beginning and end of inflation. We follow closely the derivation considered in Ref. [23] for each one of these dynamical phases and which the detailed analysis was provided. As in the previous references analyzing the dynamics of inflation after the bounce, we will always be assuming that the bounce is dominated by the kinetic energy of the inflaton (which is in fact a natural condition when the initial conditions are taken deep in the contracting phase as shown in Ref. [23]). Since the kinetic energy evolves like a stiff fluid,  $\dot{\phi}^2 \propto 1/a^6$ , it will generically dominate over the potential energy density at the bounce when starting with initial conditions for the inflaton deep in the contracting phase. Below we will summarize the main equations for each one of the phase that will be important for our study.

#### A. Setting the initial conditions in the contracting phase

We set the initial conditions in the classical contracting phase at some instant  $t$  well before the bounce time  $t_B$  and which the quantum effects are still negligible. In this case, the Hubble parameter can be expressed as

$$H \simeq \frac{1 + \beta}{3(t - t_B)}, \quad (3.4)$$

where  $\beta$  defines here the ratio between potential and kinetic energy densities for the scalar field,  $\beta = V/(\dot{\phi}^2/2)$ . On the other hand, as shown in Ref. [23],  $t - t_B$  can also be expressed as

$$t_\beta - t_B = -\frac{1 + \bar{\beta}}{3} \sqrt{\frac{3m_{\text{Pl}}^4 \bar{\beta}}{8\pi(1 + \bar{\beta})V(\phi_\beta)}}, \quad (3.5)$$

where  $\phi_\beta \equiv \phi(t_\beta)$  and  $\bar{\beta}$  is taken as the ‘‘average’’ value for  $\beta$  and we approximate it as a constant within the range  $(0, 1)$  (see Ref. [23] for details). Here, the choice of  $\beta$  parameterizes how far in the past we set the initial conditions for the inflaton field. Once the potential  $V(\phi)$  is specified,  $\phi_\beta$  is obtained by the solution of

$$\frac{V(\phi_\beta)}{V'(\phi_\beta)} = \frac{\sqrt{1 + \bar{\beta}}}{4\sqrt{3\pi}} m_{\text{Pl}}. \quad (3.6)$$

As shown in Ref. [23] (for a similar earlier prescription, see also Ref. [16]), there is one value of  $\bar{\beta}$  that can be fixed once and for all for all potentials, given by  $\bar{\beta} = 1/3$  and which is the value we will be using throughout our analysis.

#### B. The bounce phase

The solution  $\phi_\beta$  can be connected with the one valid around the bounce phase. As at the bounce phase we generically expect  $\dot{\phi}^2/2 \gg V$ , thus leading to

$$\ddot{\phi} + 3H\dot{\phi} \approx 0, \quad (3.7)$$

and we can solve Eq. (3.7) when using (3.1), with the initial condition  $\phi(t_B) = \phi_B$ , to obtain [10]

$$\phi(t) = \phi_B \pm \frac{m_{\text{Pl}}}{2\sqrt{3\pi}} \operatorname{arcsinh} \left[ \sqrt{\frac{24\pi\rho_{\text{cr}}}{m_{\text{Pl}}^4}} \frac{(t - t_B)}{t_{\text{Pl}}} \right]. \quad (3.8)$$

As shown in Ref. [23], the solution given by Eq. (3.8) holds well even deep in the contracting phase. This allows to determine  $\phi_B$  once  $\phi_\beta$  is obtained.

#### C. The postbounce preinflationary phase

After the bounce, in the expanding phase the kinetic energy of the inflaton dilutes faster than its potential energy. We denote this phase, that lasts from the

bounce instant  $t_B$  up to the transition point  $t_{tr}$ , where the potential energy equates to the kinetic energy (i.e.  $\dot{\phi}^2(t_{tr})/2 = V(\phi(t_{tr}))$ , or  $w = 0$ ), as the postbounce preinflationary phase. The inflaton's amplitude in the transition time is

$$\phi(t_{tr}) = \phi_B + \frac{m_{\text{Pl}}}{2\sqrt{3}\pi} \operatorname{arcsinh} \left[ \sqrt{\frac{24\pi\rho_{\text{cr}}}{m_{\text{Pl}}^4} \frac{(t_{tr} - t_B)}{t_{\text{Pl}}}} \right]. \quad (3.9)$$

and the time at this transition point  $t_{tr}$  is determined by solving

$$\dot{\phi}(t_{tr}) = \sqrt{2V(\phi(t_{tr}))}, \quad (3.10)$$

where we choose the convention of positive sign in both Eqs. (3.8) and (3.10) as explained in Ref. [23]. We note that explicit analytical expressions for both  $t_{tr} - t_B$  and  $\phi(t_{tr})$  can be obtained from these equations by approximating them by considering that  $t_{tr} - t_B \gg t_{\text{Pl}}$  as shown in Ref. [10]. However, these expressions are in general too complicated and since Eq. (3.10) is valid for any potential, it is simpler just to directly solve it numerically, as we do here.

## D. The inflationary phase

Soon after the transition phase, inflation starts. The instant of the start of the accelerating inflationary regime,  $t_i$ , is given when  $w = -1/3$ , i.e. when  $\dot{\phi}_i^2 = V(\phi_i)$ . The time interval between the transition phase and the beginning of inflation has been shown to be very short [10], lasting much less than one  $e$ -fold and can be neglected. This allows us to obtain  $\phi_i \equiv \phi(t_i)$  as

$$\phi_i \simeq \phi_{tr} + \dot{\phi}_{tr} t_{tr} \ln \frac{t_i}{t_{tr}}. \quad (3.11)$$

Finally, from the slow-roll coefficient  $\epsilon_V$ ,

$$\epsilon_V = \frac{1}{16\pi m_{\text{Pl}}^2} \left( \frac{V'}{V} \right)^2, \quad (3.12)$$

we determine the inflation amplitude at the end of inflation,  $\phi_{\text{end}}$ , by setting  $\epsilon_V = 1$ . For the  $\alpha$ -attractor class of potentials considered here, Eq. (2.1), we obtain that

$$\phi_{\text{end}} = 4\sqrt{3\pi\alpha} m_{\text{Pl}} \operatorname{arccoth} \left[ \frac{1}{2} \left( n + \sqrt{3\alpha} + \sqrt{(-2+n)^2 + 2n\sqrt{3\alpha} + 3\alpha} \right) \right]. \quad (3.13)$$

The total number of  $e$ -folds of inflation is then given by

$$N_{\text{inff}} \approx \frac{8\pi}{m_{\text{Pl}}^2} \int_{\phi_{\text{end}}}^{\phi_i} \frac{V}{V'} d\phi. \quad (3.14)$$

## IV. RESULTS

Let us now present our results obtained from the analysis of the  $\alpha$ -attractor models considered here. As a preliminary analysis, we consider the case where the initial conditions are set at the bounce instant  $t_B$ , according to the philosophy adopted in Refs. [15, 27] in the study using these type of inflaton potential. This will allow us to confront how well the analytical results produced for these potentials performs when compared with the numerical ones, obtained by a direct numerical solution of the background evolution equation for the inflaton, Eq. (3.3), with the modified Friedmann equation (3.1) in LQC. Note that in this case, we set arbitrary values for the inflaton amplitude  $\phi_B$  at the bounce, but still subjected to the condition that at the bounce the kinetic energy would dominate over the potential energy of the inflaton,  $\dot{\phi}_B^2/2 \gg V(\phi_B)$ . After this preliminary study, we will follow the philosophy that the initial conditions should be taken deep in the contracting phase and follow

the dynamics from this point on up to the end of inflation. In this case, we follow the methodology presented in Ref. [23] and summarized in the previous section. In these first two analysis, we work with a Barbero-Immirzi parameter that is fixed at the value  $\gamma = 0.2375$  as motivated by black hole thermodynamic studies. Finally, we will let  $\gamma$  vary and determine how the dynamics of the  $\alpha$ -attractor models can lead to constraints on its value when confronted with the observations.

### A. Initial conditions set at the bounce

By setting the initial conditions at the bounce, we fix  $\phi_B$  and then using Eqs. (3.8), (3.10), (3.11) and (3.13), we evaluate the inflaton's amplitude at the transition point, at the beginning and at the end of inflation. We denote these results as being the analytical ones. The assumed value for  $\phi_B$  is such that the number of  $e$ -folds produced are not too large and, thus, we can better control the numerical solution as far precision and time of evaluation are concerned. Then, the numerical results are obtained by using the same value for  $\phi_B$ , but numerically evolving Eq. (3.3) with the Friedmann equation (3.1) and obtained in Ref. [27]. We also choose the initial conditions such that the evolution is always at the flatter region of the  $\alpha$ -attractor models (see Fig. 1), i.e.,  $\phi_B > 0$  and  $\dot{\phi}_B > 0$ .

TABLE I. Comparison between the numeric and analytic solution for T ( $n = 0$ ), E ( $n = 1$ ) and  $n = 2$   $\alpha$ -attractor models.

model	$\phi_B/m_{\text{Pl}}$	$\phi_{\text{tr}}/m_{\text{Pl}}$	$\phi_i/m_{\text{Pl}}$	$N_{\text{infl}}$
$n = 0$ (numeric)	0.10	2.35	2.39	178.3 (144.3)
$n = 0$ (analytic)	0.10	2.38	2.44	158.5
$n = 1$ (numeric)	0.10	2.37	2.41	355.1 (287.0)
$n = 1$ (analytic)	0.10	2.40	2.46	316.2
$n = 2$ (numeric)	0.10	2.34	2.38	210.4 (172.1)
$n = 2$ (analytic)	0.10	2.38	2.43	162.7

TABLE II. The predicted results for  $\phi_B$ ,  $\phi_{\text{tr}}$ ,  $\phi_i/m_{\text{Pl}}$  and  $N_{\text{infl}}$  for the three forms of the  $\alpha$ -attractor models.

Models	$\phi_B/m_{\text{Pl}}$	$\phi_{\text{tr}}/m_{\text{Pl}}$	$\phi_i/m_{\text{Pl}}$	$N_{\text{infl}}$
T-model ( $\alpha = 5$ )	2.69	4.97	5.02	$1.84 \times 10^4$
E-model ( $\alpha = 5$ )	2.62	4.92	4.97	$3.36 \times 10^4$
$n = 2$ model ( $\alpha = 30$ )	2.62	4.89	4.95	$8.87 \times 10^3$

The results for each of the corresponding phases and the number of  $e$ -folds for the inflationary phase for the T-model ( $n = 0$ ), E-model ( $n = 1$ ) and for the  $n = 2$   $\alpha$ -attractor models are shown in Table I. To obtain these results, we have considered the parameter value  $\alpha$  for each model as set to  $\alpha_{n=0} = 5$ ,  $\alpha_{n=1} = 5$  and  $\alpha_{n=2} = 30$ , whose values are consistent with the ones given by the upper bounds given in Eq. (2.6). The normalization  $V_0$  for each potential is computed according to App. A and always at the  $N_* = 50$  value for definiteness.

In the Table I, the result for  $N_{\text{infl}}$  in parenthesis for the numerical results indicate the inflationary number of  $e$ -folds computed according to the slow-roll approximation Eq. (3.14), whose formula we also used when estimating the analytical results. The number of  $e$ -folds without the parenthesis are obtained when we follow the exact slow-roll coefficient  $\epsilon_H = -\dot{H}/H^2$  when it first becomes equal to one in the expanding phase after the bounce (e.g.,  $w_\phi = -1/3$ ) and when it gets equal to one again later at the end of inflation. As noticed by the results shown in Table I, the largest differences come from the obtained number of  $e$ -folds in each method. The slow-roll formula Eq. (3.14) produces results with a difference between the analytic and numerical results that is of order of 10%.

### B. Initial conditions set in the far past in the contracting phase

We now consider the line of thought that the appropriate moment to take the initial conditions should be deep inside the contracting phase before the bounce [18–22]. Then here we consider the evolution of the inflaton field since this moment up to the end of inflation, according to the method explained in Ref. [23] and summarized in the previous section, Sec III. As shown in Ref. [23], provided the initial conditions are set sufficiently far back in the contracting phase, the bounce will always be dominated

by the kinetic energy of the inflaton, which always grow much faster than the energy density in the potential of the inflaton. This then allows to uniquely compute and determine the evolution of the inflaton up to the end of inflation. In particular, the total number of  $e$ -folds of inflation  $N_{\text{infl}}$  becomes a predicted quantity for a given potential. The obtained results for the  $\alpha$ -attractor potentials considered in this work are shown in Table II. Here, we once again fixed the Barbero-Immirzi parameter at the value  $\gamma = 0.2375$  and considered the values for the parameter  $\alpha$  as given in the previous analysis above,  $\alpha_{n=0} = 5$ ,  $\alpha_{n=1} = 5$  and  $\alpha_{n=2} = 30$ . The cases of varying  $\alpha$  and  $\gamma$  will also be considered below.

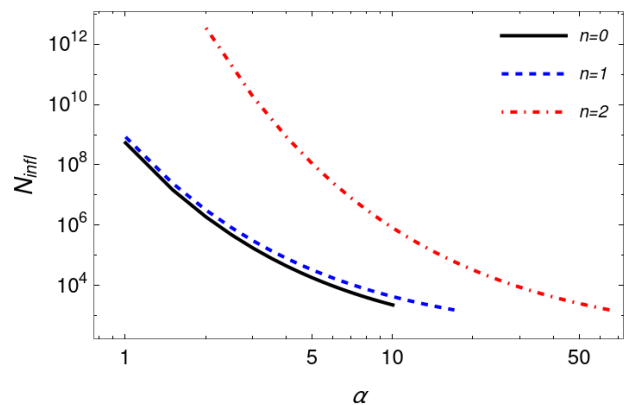


FIG. 2. Number of inflationary  $e$ -folds  $N_{\text{infl}}$  for the  $\alpha$ -attractor potentials as a function of the  $\alpha$  parameter. The Barbero-Immirzi parameter is kept at the value  $\gamma = 0.2375$ . The upper values of  $\alpha$  considered for each model follow from Eq. (2.6).

In Fig. 2, we still consider the Barbero-Immirzi parameter fixed at  $\gamma = 0.2375$ , but study how the results for

the number of  $e$ -folds of inflation  $N_{\text{infl}}$  changes by varying the parameter  $\alpha$  for each model. The maximum value for  $\alpha$  for each model is taken as given by the upper bounds given in Eq. (2.6) such that the  $\alpha$ -attractor models are consistent with the observations.

We note from the results shown in Fig. 2 that the smaller is the parameter  $\alpha$ , the larger is the number of  $e$ -folds predicted for each model. This is consistent with the fact that the smaller is  $\alpha$  the flat region of the potentials gets flatter, thus generically leading to larger number of  $e$ -folds of inflation.

### C. Varying the Barbero-Immirzi parameter

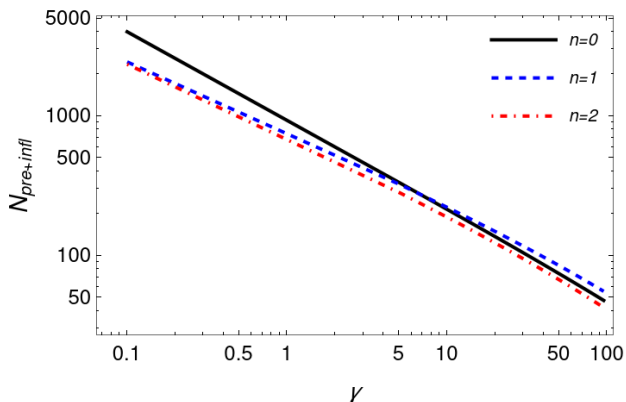


FIG. 3. Number of  $e$ -folds of evolution from the bounce up to the end of inflation,  $N_{\text{pre+infl}}$  as a function of the Barbero-Immirzi parameter  $\gamma$ . The parameter  $\alpha$  in the potential is kept fixed at the values saturating the bound given by Eq. (2.6) for each model.

Finally, we now consider the effect of varying the Barbero-Immirzi parameter  $\gamma$ . As seen from the results of Fig. 2, small values of  $\alpha$  will always lead to larger number of  $e$ -folds. Since the number of  $e$ -folds of inflation has necessarily a lower bound set by the requirement of inflation to solve the usual flatness and horizon problems of the hot big bang model, we fix  $\alpha$  in each model such as to saturate the upper bound given by Eq. (2.6). The corresponding results are given in Fig. 3.

Note that in Fig. 3 we show the total number of  $e$ -folds from the bounce up to the end of inflation,  $N_{\text{pre+infl}}$ , i.e., we also consider the duration of the pre-inflationary post-bounce phase. Here, we can take advantage of the fact that the linear perturbations in LQC are known analytically [10]. In particular, from the knowledge of the perturbations spectra in LQC, it has been shown in Ref. [23] that there is an upper bound for the Barbero-Immirzi parameter determined by the condition on  $N_{\text{pre+infl}}$ ,

$$N_{\text{pre+infl}} \gtrsim 79 - \frac{3}{2} \ln(\gamma). \quad (4.1)$$

This allows us to find that the consistency of the perturbations spectra in LQC for the  $\alpha$ -attractor models considered here with the observations then leads the following upper bounds on  $\gamma$ :

$$\gamma \lesssim \begin{cases} 51.2, & \text{for } n = 0, \\ 63.4, & \text{for } n = 1, \\ 64.2, & \text{for } n = 2, \end{cases} \quad (4.2)$$

such that larger values of  $\gamma$  than these bounds would violate Eq. (4.1).

## V. CONCLUSIONS

In this paper, we have revisited some of the results concerning a class of  $\alpha$ -attractor potentials in the context of LQC. We have considered the background evolution for these type of potentials by following the dynamics when setting the initial conditions at the bounce and also in the deep contracting phase before the bounce. The latter case has been claimed in the recent literature to be the correct point where the initial conditions should be set. It has been shown in several references [18–22] that in this case the inflationary evolution can be predicted. By taking advantage of the results obtained in Ref. [23], we have studied the dynamics of the  $\alpha$ -attractor models when varying the potential parameter  $\alpha$  and also the Barbero-Immirzi parameter  $\gamma$ . By contrasting the results with the observations, we were able to put constraints on both of these parameters. In particular, the tensor-to-scalar ratio imposes the upper bounds in the  $\alpha$  parameter as being,  $\alpha_{n=0} \lesssim 10$ ,  $\alpha_{n=1} \lesssim 17$  and  $\alpha_{n=2} \lesssim 67$ , for the  $\alpha$ -attractors T-, E- and  $n = 2$  models, respectively.

Our results have also shown that by decreasing the  $\alpha$  parameter, the number of  $e$ -folds predicted for each model in LQC increases. Likewise, the lower is the value for the Barbero-Immirzi parameter, the larger is also the number of  $e$ -folds of inflation. Then, by a previous general bound determined in Ref. [23] and set on the total duration of the pre-inflationary postbounce and later inflationary phases in LQC, we were able to find the further upper bounds for the the Barbero-Immirzi parameter for the  $\alpha$ -attractor models:  $\gamma_{n=0} \lesssim 51.2$ ,  $\gamma_{n=1} \lesssim 63.4$  and  $\gamma_{n=2} \lesssim 64.2$ . Our results show that when we combine constraints on the observables and predictions about the duration of inflation in LQC, general bounds can be set on the  $\alpha$ -attractor potentials and also on the Barbero-Immirzi parameter.

## VI. ACKNOWLEDGEMENTS

G.L.L.W.L. acknowledges financial support of the Coordenação de Aperfeiçoamento de Pessoal de Nível Superior (CAPES). R.O.R. acknowledges financial support by research grants from Conselho Nacional de Desenvolvimento Científico e Tecnológico (CNPq), Grant No.

307286/2021-5, and from Fundação Carlos Chagas Filho de Amparo à Pesquisa do Estado do Rio de Janeiro (FAPERJ), Grant No. E-26/201.150/2021.

## Appendix A

The normalization  $V_0$  of the inflaton potential is fixed by the amplitude of the CMB primordial scalar of curvature power spectrum  $\Delta_{\mathcal{R}}$ , given by [52]

$$\Delta_{\mathcal{R}} = \left( \frac{H_*^2}{2\pi\dot{\phi}_*} \right)^2, \quad (\text{A1})$$

where a subindex \* means that the quantities are evaluated at the Hubble radius crossing  $k_*$  ( $k_* = a_*H_*$ ), which typically happens around  $N_* \sim 50 - 60$   $e$ -folds before the end of inflation. From the Planck collaboration [53],  $\ln(10^{10}\Delta_{\mathcal{R}}) \simeq 3.047$  (TT,TE,EE-lowE+lensing+BAO 68% limits). During the slow-roll regime of inflation, we have  $H^2 \simeq 8\pi V/(3m_{\text{Pl}}^2)$  and  $\dot{\phi} \simeq -V_{,\phi}/(3H)$ , which then gives for Eq. (A1) the result

$$\Delta_{\mathcal{R}} \simeq \frac{128\pi}{3m_{\text{Pl}}^6} \frac{V_*^3}{V_{,\phi_*}^2}. \quad (\text{A2})$$

By fixing  $N_*$ , we can determine  $\phi_*$  by solving the number of  $e$ -folds equation,

$$N_* = \frac{8\pi}{m_{\text{Pl}}^2} \int_{\phi_{\text{end}}}^{\phi_*} \frac{V}{V'} d\phi. \quad (\text{A3})$$

For the  $\alpha$ -attractor class of potentials considered here, Eq. (2.1),  $\phi_{\text{end}}$  is given by Eq. (3.13) and  $N_*$  is found to be given by

$$\begin{aligned} N_* = & \frac{3\alpha}{4n(n-2)^2} \{2b(n-2)^2 - (n-2)[n(e^{2b} - y_*)] \\ & + (n-2)\ln(y_*) - 4(n-1)(\ln[e^{2b}(n-2) + n] \\ & - \ln(n + 2y_* - ny_*))\}, \end{aligned} \quad (\text{A4})$$

where we have defined

$$y_* = e^{\frac{2}{3\alpha} \frac{\phi_*}{m_{\text{Pl}}}}, \quad (\text{A5})$$

$$b = \text{arccoth}(a_n), \quad (\text{A6})$$

and

$$a_n = \frac{1}{2} \left[ n + \sqrt{3\alpha} + \sqrt{(n-2)^2 + 2n\sqrt{3\alpha} + 3\alpha} \right]. \quad (\text{A7})$$

From Eq. (A4), we then find that for the T-model ( $n = 0$ ) that

$$\phi_*^{n=0} = \frac{m_{\text{Pl}}}{4} \sqrt{\frac{3\alpha}{\pi}} \text{ArcCosh} \left[ \frac{4N_*}{3\alpha} - \frac{1+a_0^2}{1-a_0^2} \right], \quad (\text{A8})$$

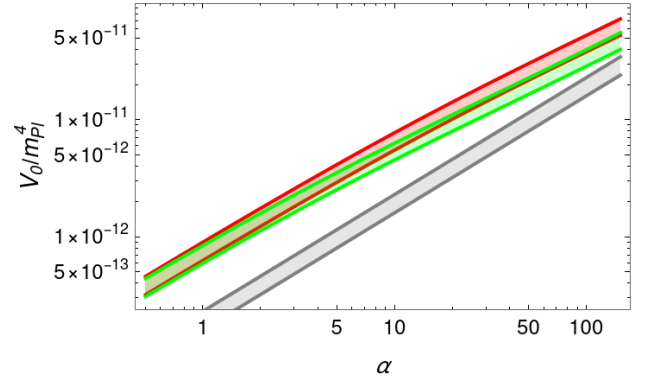


FIG. 4. The normalization  $V_0$  for the  $\alpha$ -attractor potentials models considered in this work. The gray, green and red curves and respective regions are for the T-model ( $n = 0$ ), E-model ( $n = 1$ ) and  $n = 2$   $\alpha$ -attractor models, respectively. They are obtained by fixing  $N_*$  in the values  $N_* = 50$  (upper curve) and  $N_* = 60$  (lower curve).

for the E-model ( $n = 1$ ), we have that

$$\begin{aligned} \phi_*^{n=1} = & \sqrt{\frac{3\alpha}{\pi}} \frac{m_{\text{Pl}}}{4} \left\{ \frac{1 + 2\text{arccoth}(a_1)}{a_1 - 1} \right. \\ & - W_{-1} \left[ \frac{e^{-1 + \frac{2}{a_1 - 1} - \frac{4N_*}{3\alpha}} (1 + a_1)}{a_1 - 1} \right] \\ & - \frac{4N_*}{3(a_1 - 1)\alpha} \\ & \left. + \frac{a_1}{a_1 - 1} \left( 1 - 2\text{arccoth}(a_1) + \frac{4N_*}{3\alpha} \right) \right\}, \end{aligned} \quad (\text{A9})$$

and for  $n = 2$ , we have that

$$\begin{aligned} \phi_*^{n=2} = & \frac{m_{\text{Pl}}}{24\sqrt{\pi\alpha}} \left\{ -12\sqrt{\alpha} - 16\sqrt{3}N_* \right. \\ & + 3\sqrt{3}\alpha(-1 + 4\text{arccoth}(a_2)) \\ & \left. - W_{-1} \left[ -e^{-1 - \frac{4}{\sqrt{3}\sqrt{\alpha}} + 4\text{arccoth}(a_2) - \frac{16N_*}{3\alpha}} \right] \right\}, \end{aligned} \quad (\text{A10})$$

where in the above equations,  $W_{-1}(x)$  is the Lambert function.

Note that the above equations depend on the value of  $\alpha$ . In Fig. 4 we show the potential normalization  $V_0$  as a function of  $\alpha$  when making use of Eq. (A2).

The use of the tensor-to-scalar ratio  $r$  and the spectral tilt  $n_s$  of the scalar spectrum allows us to find an upper bound for the parameter  $\alpha$  for each of the potentials considered here.  $r$  and  $n_s$  are defined by [52]

$$r = 16\epsilon_V, \quad (\text{A11})$$

and

$$n_s = 1 - 6\epsilon_V + 2\eta_V, \quad (\text{A12})$$



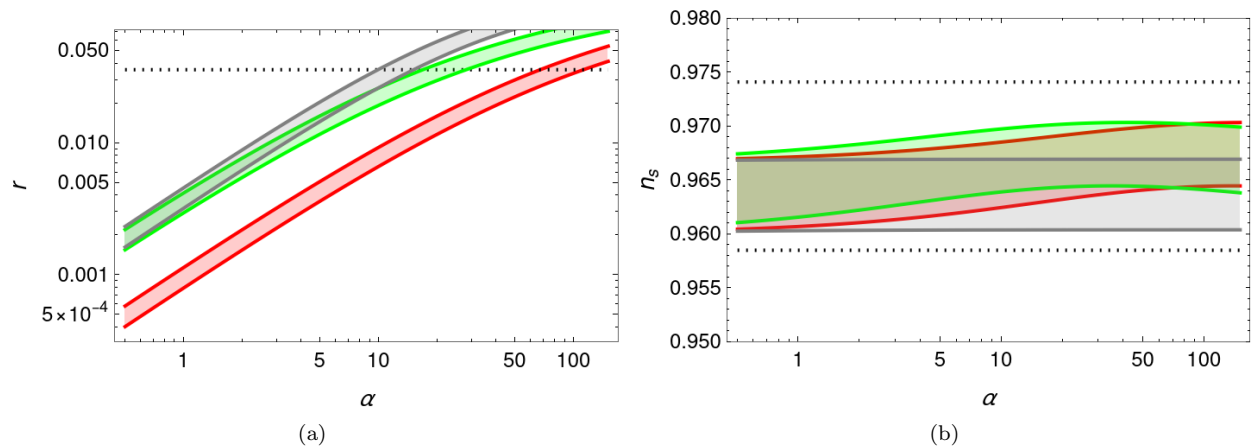


FIG. 5. The tensor-to-scalar ratio (panel a) and the spectral tilt (panel b) for the  $\alpha$ -attractor potential models considered in this work. The gray, green and red curves and respective regions are for the T-model ( $n = 0$ ), E-model ( $n = 1$ ) and  $n = 2$   $\alpha$ -attractor models, respectively. The upper curves correspond to  $N_* = 50$ , while the lower curves are for  $N_* = 60$ . The horizontal dotted lines mark the upper bound for  $r$  (given by Eq. (2.5)) and the upper and lower ranges at  $2\text{-}\sigma$  for  $n_s$ .

where  $\epsilon_V$  and  $\eta_V$  are the slow-roll coefficients:

$$\epsilon_V = \frac{1}{16\pi m_{\text{Pl}}^2} \left( \frac{V'}{V} \right)^2, \quad \eta_V = \frac{1}{8\pi m_{\text{Pl}}^2} \frac{V''}{V}, \quad (\text{A13})$$

and which are evaluated at the value  $\phi_*$ .

From the expressions (A8) – (A10), we evaluate both

$r$  and  $n_s$  for the fiducial values of  $N_* = 50$  and  $N_* = 60$  as a function of  $\alpha$ . The results are shown in Fig. 5. For  $\alpha \ll 1$ , the results approach the ones given in Eqs. (2.3) and (2.2), for  $r$  and  $n_s$ , respectively. For  $\alpha > 1$ , the tensor-to-scalar ratio gives the stronger constrain on the value for  $\alpha$  for each type of potential, leading to the values given in Eq. (2.6).

- 
- [1] A. Ashtekar and J. Lewandowski, Background independent quantum gravity: A Status report, *Class. Quant. Grav.* **21**, R53 (2004) doi:10.1088/0264-9381/21/15/R01 [arXiv:gr-qc/0404018 [gr-qc]].
- [2] A. Ashtekar and P. Singh, Loop Quantum Cosmology: A Status Report, *Class. Quant. Grav.* **28**, 213001 (2011) doi:10.1088/0264-9381/28/21/213001 [arXiv:1108.0893 [gr-qc]].
- [3] C. Rovelli and F. Vidotto, *Covariant Loop Quantum Gravity: An Elementary Introduction to Quantum Gravity and Spinfoam Theory*, Cambridge University Press, 2014, ISBN 978-1-107-06962-6, 978-1-316-14729-0
- [4] A. Ashtekar, M. Bojowald and J. Lewandowski, Mathematical structure of loop quantum cosmology, *Adv. Theor. Math. Phys.* **7**, no.2, 233-268 (2003) doi:10.4310/ATMP.2003.v7.n2.a2 [arXiv:gr-qc/0304074 [gr-qc]].
- [5] M. Bojowald, Loop quantum cosmology, *Living Rev. Rel.* **8**, 11 (2005) doi:10.12942/lrr-2005-11 [arXiv:gr-qc/0601085 [gr-qc]].
- [6] A. Ashtekar, T. Pawłowski and P. Singh, Quantum nature of the big bang, *Phys. Rev. Lett.* **96**, 141301 (2006) doi:10.1103/PhysRevLett.96.141301 [arXiv:gr-qc/0602086 [gr-qc]].
- [7] A. Ashtekar and D. Sloan, Loop quantum cosmology and slow roll inflation, *Phys. Lett. B* **694**, 108-112 (2011) doi:10.1016/j.physletb.2010.09.058 [arXiv:0912.4093 [gr-qc]].
- [8] A. Barrau, T. Cailleteau, J. Grain and J. Mielczarek, Observational issues in loop quantum cosmology, *Class. Quant. Grav.* **31**, 053001 (2014) doi:10.1088/0264-9381/31/5/053001 [arXiv:1309.6896 [gr-qc]].
- [9] I. Agullo and P. Singh, Loop Quantum Cosmology, doi:10.1142/9789813220003-0007 [arXiv:1612.01236 [gr-qc]].
- [10] T. Zhu, A. Wang, G. Cleaver, K. Kirsten and Q. Sheng, Pre-inflationary universe in loop quantum cosmology, *Phys. Rev. D* **96**, no.8, 083520 (2017) doi:10.1103/PhysRevD.96.083520 [arXiv:1705.07544 [gr-qc]].
- [11] M. Shahalam, M. Sharma, Q. Wu and A. Wang, Preinflationary dynamics in loop quantum cosmology: Power-law potentials, *Phys. Rev. D* **96**, no.12, 123533 (2017) doi:10.1103/PhysRevD.96.123533 [arXiv:1710.09845 [gr-qc]].
- [12] B. F. Li, P. Singh and A. Wang, Qualitative dynamics and inflationary attractors in loop cosmology, *Phys. Rev. D* **98**, no.6, 066016 (2018) doi:10.1103/PhysRevD.98.066016 [arXiv:1807.05236 [gr-qc]].
- [13] M. Sharma, M. Shahalam, Q. Wu and A. Wang, Preinflationary dynamics in loop quantum cosmology: Monodromy Potential, *JCAP* **11**, 003 (2018) doi:10.1088/1475-7516/2018/11/003 [arXiv:1808.05134 [gr-qc]].
- [14] B. F. Li, P. Singh and A. Wang, Genericness of



- pre-inflationary dynamics and probability of the desired slow-roll inflation in modified loop quantum cosmologies, *Phys. Rev. D* **100**, no.6, 063513 (2019) doi:10.1103/PhysRevD.100.063513 [arXiv:1906.01001 [gr-qc]].
- [15] M. Shahalam, M. Al Ajmi, R. Myrzakulov and A. Wang, Revisiting pre-inflationary Universe of family of  $\alpha$ -attractor in loop quantum cosmology, *Class. Quant. Grav.* **37**, no.19, 195026 (2020) doi:10.1088/1361-6382/aba486 [arXiv:1912.00616 [gr-qc]].
- [16] A. Ashtekar and D. Sloan, Probability of Inflation in Loop Quantum Cosmology, *Gen. Rel. Grav.* **43**, 3619-3655 (2011) doi:10.1007/s10714-011-1246-y [arXiv:1103.2475 [gr-qc]].
- [17] L. L. Graef and R. O. Ramos, Probability of Warm Inflation in Loop Quantum Cosmology, *Phys. Rev. D* **98**, no.2, 023531 (2018) doi:10.1103/PhysRevD.98.023531 [arXiv:1805.05985 [gr-qc]].
- [18] L. Linsefors and A. Barrau, Duration of inflation and conditions at the bounce as a prediction of effective isotropic loop quantum cosmology, *Phys. Rev. D* **87**, no.12, 123509 (2013) doi:10.1103/PhysRevD.87.123509 [arXiv:1301.1264 [gr-qc]].
- [19] L. Linsefors and A. Barrau, Exhaustive investigation of the duration of inflation in effective anisotropic loop quantum cosmology, *Class. Quant. Grav.* **32**, no.3, 035010 (2015) doi:10.1088/0264-9381/32/3/035010 [arXiv:1405.1753 [gr-qc]].
- [20] B. Bolliet, A. Barrau, K. Martineau and F. Moulin, Some Clarifications on the Duration of Inflation in Loop Quantum Cosmology, *Class. Quant. Grav.* **34**, no.14, 145003 (2017) doi:10.1088/1361-6382/aa7779 [arXiv:1701.02282 [gr-qc]].
- [21] K. Martineau, A. Barrau and S. Schander, Detailed investigation of the duration of inflation in loop quantum cosmology for a Bianchi-I universe with different inflation potentials and initial conditions, *Phys. Rev. D* **95**, no.8, 083507 (2017) doi:10.1103/PhysRevD.95.083507 [arXiv:1701.02703 [gr-qc]].
- [22] L. N. Barboza, L. L. Graef and R. O. Ramos, Warm bounce in loop quantum cosmology and the prediction for the duration of inflation, *Phys. Rev. D* **102**, no.10, 103521 (2020) doi:10.1103/PhysRevD.102.103521 [arXiv:2009.13587 [gr-qc]].
- [23] L. N. Barboza, G. L. L. W. Levy, L. L. Graef and R. O. Ramos, Constraining the Barbero-Immirzi parameter from the duration of inflation in loop quantum cosmology, *Phys. Rev. D* **106**, no.10, 103535 (2022) doi:10.1103/PhysRevD.106.103535 [arXiv:2206.14881 [gr-qc]].
- [24] R. Kallosh and A. Linde, Universality Class in Conformal Inflation, *JCAP* **07**, 002 (2013) doi:10.1088/1475-7516/2013/07/002 [arXiv:1306.5220 [hep-th]].
- [25] R. Kallosh, A. Linde and D. Roest, Superconformal Inflationary  $\alpha$ -Attractors, *JHEP* **11**, 198 (2013) doi:10.1007/JHEP11(2013)198 [arXiv:1311.0472 [hep-th]].
- [26] R. Kallosh, A. Linde and D. Roest, Universal Attractor for Inflation at Strong Coupling, *Phys. Rev. Lett.* **112**, no.1, 011303 (2014) doi:10.1103/PhysRevLett.112.011303 [arXiv:1310.3950 [hep-th]].
- [27] M. Shahalam, M. Sami and A. Wang, Preinflationary dynamics of  $\alpha$ -attractor in loop quantum cosmology, *Phys. Rev. D* **98**, no.4, 043524 (2018) doi:10.1103/PhysRevD.98.043524 [arXiv:1806.05815 [astro-ph.CO]].
- [28] Y. Akrami *et al.* [Planck], Planck 2018 results. X. Constraints on inflation, *Astron. Astrophys.* **641**, A10 (2020) doi:10.1051/0004-6361/201833887 [arXiv:1807.06211 [astro-ph.CO]].
- [29] N. Aghanim *et al.* [Planck], Planck 2018 results. V. CMB power spectra and likelihoods, *Astron. Astrophys.* **641**, A5 (2020) doi:10.1051/0004-6361/201936386 [arXiv:1907.12875 [astro-ph.CO]].
- [30] A. A. Starobinsky, A New Type of Isotropic Cosmological Models Without Singularity, *Phys. Lett. B* **91**, 99-102 (1980) doi:10.1016/0370-2693(80)90670-X
- [31] E. V. Linder, Dark Energy from  $\alpha$ -Attractors, *Phys. Rev. D* **91**, no.12, 123012 (2015) doi:10.1103/PhysRevD.91.123012 [arXiv:1505.00815 [astro-ph.CO]].
- [32] M. Shahalam, R. Myrzakulov, S. Myrzakul and A. Wang, Observational constraints on the generalized  $\alpha$  attractor model, *Int. J. Mod. Phys. D* **27**, no.05, 1850058 (2018) doi:10.1142/S021827181850058X [arXiv:1611.06315 [astro-ph.CO]].
- [33] D. I. Kaiser and E. I. Sfakianakis, Multifield Inflation after Planck: The Case for Nonminimal Couplings, *Phys. Rev. Lett.* **112**, no.1, 011302 (2014) doi:10.1103/PhysRevLett.112.011302 [arXiv:1304.0363 [astro-ph.CO]].
- [34] R. Kallosh, A. Linde and D. Roest, Large field inflation and double  $\alpha$ -attractors, *JHEP* **08**, 052 (2014) doi:10.1007/JHEP08(2014)052 [arXiv:1405.3646 [hep-th]].
- [35] K. Dimopoulos and C. Owen, Quintessential Inflation with  $\alpha$ -attractors, *JCAP* **06**, 027 (2017) doi:10.1088/1475-7516/2017/06/027 [arXiv:1703.00305 [gr-qc]].
- [36] J. J. M. Carrasco, R. Kallosh and A. Linde,  $\alpha$ -Attractors: Planck, LHC and Dark Energy, *JHEP* **10**, 147 (2015) doi:10.1007/JHEP10(2015)147 [arXiv:1506.01708 [hep-th]].
- [37] A. R. Liddle and S. M. Leach, How long before the end of inflation were observable perturbations produced?, *Phys. Rev. D* **68**, 103503 (2003) doi:10.1103/PhysRevD.68.103503 [arXiv:astro-ph/0305263 [astro-ph]].
- [38] P. A. R. Ade *et al.* [BICEP and Keck], Improved Constraints on Primordial Gravitational Waves using Planck, WMAP, and BICEP/Keck Observations through the 2018 Observing Season, *Phys. Rev. Lett.* **127**, no.15, 151301 (2021) doi:10.1103/PhysRevLett.127.151301 [arXiv:2110.00483 [astro-ph.CO]].
- [39] K. A. Meissner, Black hole entropy in loop quantum gravity, *Class. Quant. Grav.* **21**, 5245-5252 (2004) doi:10.1088/0264-9381/21/22/015 [arXiv:gr-qc/0407052 [gr-qc]].
- [40] J. Engle, K. Noui, A. Perez and D. Pranzetti, Black hole entropy from an SU(2)-invariant formulation of Type I isolated horizons, *Phys. Rev. D* **82**, 044050 (2010) doi:10.1103/PhysRevD.82.044050 [arXiv:1006.0634 [gr-qc]].
- [41] E. Bianchi, Entropy of Non-Extremal Black Holes from Loop Gravity, [arXiv:1204.5122 [gr-qc]].
- [42] P. J. Wong, Shape Dynamical Loop Gravity from a Conformal Immirzi Parameter, *Int. J. Mod. Phys. D* **26**,

- no.11, 1750131 (2017) doi:10.1142/S0218271817501310 [arXiv:1701.07420 [gr-qc]].
- [43] I. Agullo, A. Ashtekar and W. Nelson, A Quantum Gravity Extension of the Inflationary Scenario, *Phys. Rev. Lett.* **109**, 251301 (2012) doi:10.1103/PhysRevLett.109.251301 [arXiv:1209.1609 [gr-qc]].
- [44] M. Fernandez-Mendez, G. A. Mena Marugan and J. Olmedo, Hybrid quantization of an inflationary universe, *Phys. Rev. D* **86**, 024003 (2012) doi:10.1103/PhysRevD.86.024003 [arXiv:1205.1917 [gr-qc]].
- [45] M. Benetti, L. Graef and R. O. Ramos, Observational Constraints on Warm Inflation in Loop Quantum Cosmology, *JCAP* **10**, 066 (2019) doi:10.1088/1475-7516/2019/10/066 [arXiv:1907.03633 [astro-ph.CO]].
- [46] J. B. Munoz and M. Kamionkowski, Equation-of-State Parameter for Reheating, *Phys. Rev. D* **91**, no.4, 043521 (2015) doi:10.1103/PhysRevD.91.043521 [arXiv:1412.0656 [astro-ph.CO]].
- [47] S. K. Asante, B. Dittrich and H. M. Haggard, Effective Spin Foam Models for Four-Dimensional Quantum Gravity, *Phys. Rev. Lett.* **125**, no.23, 231301 (2020) doi:10.1103/PhysRevLett.125.231301 [arXiv:2004.07013 [gr-qc]].
- [48] S. K. Asante, B. Dittrich and J. Padua-Arguelles, Effective spin foam models for Lorentzian quantum gravity, *Class. Quant. Grav.* **38**, no.19, 195002 (2021) doi:10.1088/1361-6382/ac1b44 [arXiv:2104.00485 [gr-qc]].
- [49] L. Perlov, Barbero-Immirzi value from experiment, *Mod. Phys. Lett. A* **36**, no.27, 2150192 (2021) doi:10.1142/S0217732321501923 [arXiv:2005.14141 [gr-qc]].
- [50] B. Broda and M. Szanecki, A relation between the Barbero-Immirzi parameter and the standard model, *Phys. Lett. B* **690**, 87-89 (2010) doi:10.1016/j.physletb.2010.05.004 [arXiv:1002.3041 [gr-qc]].
- [51] S. Mercuri and V. Taveras, Interaction of the Barbero-Immirzi Field with Matter and Pseudo-Scalar Perturbations, *Phys. Rev. D* **80**, 104007 (2009) doi:10.1103/PhysRevD.80.104007 [arXiv:0903.4407 [gr-qc]].
- [52] D. H. Lyth and A. R. Liddle, *The Primordial Density Perturbation: Cosmology, Inflation and the Origin of Structure* (Cambridge University Press, Cambridge, England, 2009)
- [53] N. Aghanim *et al.* [Planck], Planck 2018 results. VI. Cosmological parameters, *Astron. Astrophys.* **641**, A6 (2020) [erratum: *Astron. Astrophys.* **652**, C4 (2021)] doi:10.1051/0004-6361/201833910 [arXiv:1807.06209 [astro-ph.CO]].